Heteronuclear 1D and 2D NMR Resonances Detected by Chemical Exchange Saturation Transfer to Water

Water-Based NMR Spectroscopy

International Edition: DOI: 10.1002/anie.201611733
German Edition: DOI: 10.1002/ange.201611733

Heteronuclear 1D and 2D NMR Resonances Detected by Chemical Exchange Saturation Transfer to Water

*Ricardo P. Martinho[+], Mihajlo Novakovic[+], Gregory L. Olsen, and Lucio Frydman**

Abstract: *A method to detect NMR spectra from heteronuclei through the modulation that they impose on a water resonance is exemplified. The approach exploits chemical exchange saturation transfers, which can magnify the signal of labile protons through their influence on a water peak. To impose a heteronuclear modulation on water, an HMQC-type sequence was combined with the FLEX approach. 1D ^{15}N NMR spectra of exchanging sites could thus be detected, with about tenfold amplifications over the ^{15}N modulations afforded by conventionally detected HMQC NMR spectroscopy. Extensions of this approach enable 2D heteronuclear acquisitions on directly bonded ^{1}H–^{15}N spin pairs, also with significant signal amplification. Despite the interesting limits of detection that these signal enhancements could open in NMR spectroscopy, these gains are constrained by the rates of solvent exchange of the targeted heteronuclear pairs, as well as by spectrometer instabilities affecting the intense water resonances detected in these experiments.*

Nuclear magnetic resonance (NMR) is often hampered by its low sensitivity. Several approaches have emerged to overcome this, including hardware improvements[1] and methods for enhancing the signals of liquids and solids by nuclear hyperpolarization.[2] Foremost among the sensitivity-challenged applications of NMR is in vivo spectroscopy, where averaging times are by necessity capped and where hardware options are limited by the physical characteristics of the sample. A breakthrough in in vivo NMR spectroscopy occurred with the advent of chemical exchange saturation transfer (CEST),[3] which exploits the transfer of saturation from labile protons to water to facilitate the detection of the former in metabolites, customized contrast agents, and tissue macromolecules.[4] Instead of using a single transfer to observe the evolution of these labile sites, as in exchange spectroscopy,[5] CEST relies on prolonged, frequency-selective saturation of the labile protons, followed by a transfer of this effect to the much stronger solvent resonance. This forfeits the possibility of achieving a broadband interrogation of the full spectrum; yet this is compensated by the potential amplification of the frequency-selective information by multiple solute–solvent exchanges. Such exchanges will enhance the saturation by factors on the order of $k_{ex}\,T_1^{obs}$, where k_{ex} is the rate of solvent exchange with the labile proton, and T_1^{obs} is the relaxation time of the observed water molecules. This product can lead to orders-of-magnitude signal enhancements with respect to a single labile proton response. CEST has thus enabled the 3D NMR imaging of previously unmappable species, including glucose,[6a] urea,[6b] creatine,[7] and intrinsic proteins,[3b] and is rapidly becoming a valuable alternative for investigating health, disease, and homeostasis in both animals and humans.[6,7]

Despite these major sensitivity benefits, efforts still continue to reinstate the speed and multiplexing benefits that are common in Fourier transform (FT) NMR spectroscopy into CEST. These endeavors led to the possibility of collecting broadband spectral information by the application of suitably tuned field gradients[8] and, most relevant for the present work, by the establishment of Fourier-based alternatives for both thermally and hyperpolarized samples.[9–11] In the frequency labeled exchange (FLEX) experiment, for instance, the solute spectral region to be targeted is initially encoded by a pair of selective excitation/storage pulses separated by a delay t_1, that will modulate the amplitudes of the magnetizations of the labile sites. However, rather than observing these directly after an exchange with the solvent, FLEX loops this process numerous times, magnifying the encoding effects onto the water resonance, and imposing a modulation on the latter that is much larger than what a single mixing would afford. Repeating this as a function of t_1 and applying a single, final observation pulse on the water molecules after each encoding, enables after 2D FT the spectral detection of the labile protons with an increased sensitivity. Very recently,[12] this effect was extended by the use of an ^{15}N-selective BIRD pulse,[13] transferring the ^{15}N presence to bonded urea protons with a 0/180° amplitude modulation. By performing a ^{1}H-based FLEX experiment on the latter, a water image with a ^{15}N-encoded saturation effect of up to 25% was obtained. The present study elaborates these ideas in a related but different direction, by introducing an approach that exploits their advantages while seeking a full time-domain encoding of the heteronuclear dimension. To achieve this, the principles underlying FLEX[11] were combined with those of HMQC experiments that avoid the excitation of water.[14] This opens up new possibilities to record 1D ^{15}N NMR spectra from sites connected to labile protons as well as 2D correlation spectra between the ^{15}N nuclei and these labile hydrogen atoms. In both cases, these heteronucleus-oriented experiments ended up being observed on water, thereby benefiting from the type of sensitivity enhancement that characterizes CEST.

[*] R. P. Martinho,[+] M. Novakovic,[+] Dr. G. L. Olsen, Prof. Dr. L. Frydman
Department of Chemical Physics, Weizmann Institute of Sciences
76100 Rehovot (Israel)
E-mail: lucio.frydman@weizmann.ac.il

[+] These authors contributed equally to this work.

Supporting information and the ORCID identification number(s) for the author(s) of this article can be found under: http://dx.doi.org/10.1002/anie.201611733.

To explore these ideas further, pulse sequences for what we denominate "heteronuclear FLEX" (HetFLEX) were written (Figure 1 a), both in a 1D form encoding solely the ^{15}N evolution and as a 2D ^{15}N–^{1}H extension. To incorporate all desired elements, these sequences began with a chemical-shift-specific creation of heteronuclear $H_{\pm}N_{\pm}$ states, using selective 90° pulses that exclusively address the NH spectral region.[16] These coherences were allowed to evolve under the action of the ^{15}N chemical shift, and the resulting $\frac{\cos}{\sin}(\omega_N t_1)$ amplitude modulation was transferred back to the adjacent proton. Then, instead of detecting the ensuing transverse ^{1}H coherences as in HMQC, these were stored onto H_z as per the dictates of FLEX, and allowed to undergo exchange with the hitherto untouched magnetization of water over a mixing period t_{exch}. This procedure was repeated N times to enhance the modulation on the water up to a plateau constrained by T_1 of the water. Finally, the water signal was detected with full or partial excitation for each t_1 encoding increment, delivering the heteronucleus-imposed modulation in its amplitude. Figure S1 in the Supporting Information illustrates how the resulting modulations look like for 1D acquisitions using t_1 as the sole ^{15}N modulation variable, as well as for 2D ^{15}N/^{1}H spectral correlations employing t_1/t_2 increments. Data are also shown for experiments involving a single scan per t_1, where the desired modulations ride on top of a pedestal arising from the non-exchanged water molecules, and for two scan experiments where the water pedestal is subtracted by ^{15}N phase cycling. For both instances, quadrature components can be generated by using orthogonal pulse phases, enabling a sign discrimination of the HetFLEX resonance position. ^{15}N 1D spectra acquired after Fourier transforming signals acquired using this sequence are compared against 1D traces arising from ^{1}H-detected HMQC acquisitions performed using identical selective pulses but no water signal manipulations in Figure 1 b–e. These data confirm a per-scan increase in the ^{15}N intensity modulation upon relying on the water detection, ranging from 13 to 30 times that of HMQC. Although these are auspicious enhancements, we see that the noise in HetFLEX is also magnified, depriving the spectra from translating these signal enhancements into equal signal-to-noise ratio (SNR) gains: compared to HMQC-derived 1D ^{15}N spectra, HetFLEX SNRs are solely enhanced by a factor of 2–5. This HetFLEX noise does not appear to be thermal, but rather originate from "t_1 noise"[15] associated with the detection of a concentrated water signal in these experiments. Efforts are under way to attenuate these in-principle removable effects, by perfecting the experimental setup and by deconvolution methods. Still, it is interesting to note that comparisons between 1D ^{15}N NMR traces arising from HetFLEX and HMQC acquisitions yield remarkably similar results, not only for single amine and amide moieties, but also for more complex samples. Figure 1 d shows this similarity for a 3 kDa cutoff lysate composed of several peptides that are essentially unstructured, and hence significantly exposed to fast chemical exchange with the solvent.[16] Figure 1 e shows it for barstar, a folded 89 residue globular protein for which most ^{15}N atoms are probably not exposed to water.[17]

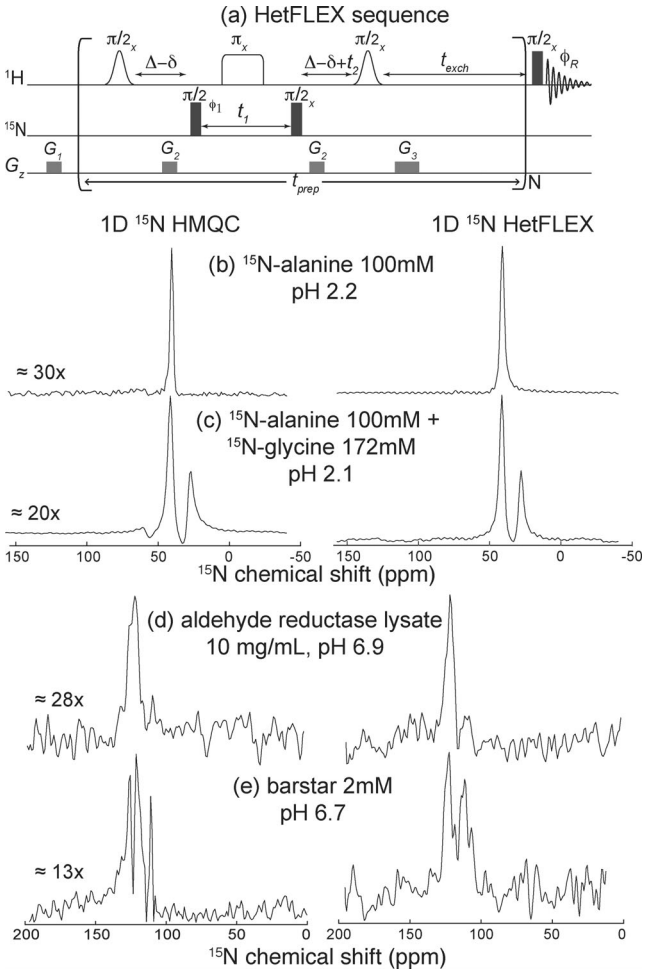

Figure 1. a) Pulse scheme of the HetFLEX experiment. t_1 and t_2 are the ^{15}N and ^{1}H encoding delays; open shapes correspond to frequency-selective 90° or 180° pulses; filled black rectangles are hard 90° pulses; G_1, G_2, and G_3 are purging gradients; Δ corresponds to $1/2J$, and δ is a factor compensating for the width of the *sinc* pulse. Following the second ^{15}N pulse, a $\Delta-\delta$ delay is used for 1D experiments, whereas for 2D experiments, t_2 is added. As a constant t_{prep} time is used for each loop within brackets, the exchange time varies slightly depending on the t_1 and t_2 increments; this is done in order to minimize relaxation weightings for different encodings. ϕ_1 was incremented by 90° to achieve quadrature detection[18] and phase-cycled as $\pm x$ together with ϕ_R to achieve water cancellation. b–e) 1D ^{15}N spectra extracted from conventional 2D HMQC (left) and HetFLEX data (right) for different ^{15}N-labeled samples. Both sequences were applied on the same samples using identical pulses and gains, the same number of t_1 increments (64), equal numbers of scans per increment (2), identical recycle delays (2 s), and equal pulses (other than for the final 90° ^{1}H pulse and purging gradient, omitted in the HMQC). The factors in the HMQC column reflect the vertical scale amplifications used to bring the HMQC traces to the same intensity as their HetFLEX counterparts. All spectra were acquired at 23.5 °C except for that of the lysate, which was collected at 37 °C; see the Supporting Information for further details.

A number of independent and interrelated parameters control the HetFLEX intensity. These include, in addition to HMQC-derived variables, the time t_{exch} and number N over which exchange loops are repeated. The signal intensities also depend on the pH and temperature, which control the exchange rate k_{ex} between labile sites and the solvent, and thereby the efficiencies of both the heteronuclear polarization

transfer and the solvent magnetization transfer processes. All these, as well as the various T_1 values involved, will determine the sensitivity and therefore the practicality of the experiment. To assess the influence of some of these parameters, a sample of alanine in D_2O/H_2O (2:8) at pH 2.2 was examined. Table 1 presents the effect of temperature on the

Table 1: Amplitudes of the ^{15}N-driven modulations [%] measured in HMQC, FLEX, and HetFLEX on aqueous alanine at different temperatures.[a]

	Temperature				
	6.5 °C	10.0 °C	17.0 °C	23.5 °C	29.5 °C
$\Delta I^{FID}_{HMQC}/I_H$ [%]	78 ± 8	70 ± 3	68 ± 0.5	17 ± 3	4.9 ± 0.9
$\Delta I^{FID}_{FLEX}/I_{water}$ [%]	3.8 ± 0.7	4.3 ± 0.1	6.4 ± 0.1	17.2 ± 0.5	13.1 ± 0.2
$\Delta I^{FID}_{HetFLEX}/I_{water}$ [%]	2.7 ± 0.3	3.5 ± 0.1	4.6 ± 0.1	3.1 ± 0.1	0.6 ± 0.1
$\Delta I^{FID}_{HMQC}\Delta I^{FID}_{FLEX}$ [%]	3.0 ± 0.6	3.0 ± 0.1	4.4 ± 0.1	2.9 ± 0.4	0.6 ± 0.1

[a] The first row compares ΔI^{FID}_{HMQC} against the thermal magnetization of the NH protons, whereas the FLEX-based experiments are compared with water; the two middle rows describe these modulations as percentages of the water signal intensity, when measured for $t_{exch} = 40$ ms and $N = 64$. The last row is the expected efficiency derived from the first two rows.

observed HetFLEX modulation, and analyzes it in terms of its two governing processes, namely the HMQC transfer efficiency and the FLEX efficiency. The former steadily degrades with temperature as a result of the increased solvent exchange rate. At the same time, the ^1H FLEX efficiency improves because of the increase in exchange rate. The overall HetFLEX outcome closely follows the product between the efficiencies observed for these two modules, $\Delta I^{FID}_{HetFLEX} = \Delta I^{FID}_{HMQC}\Delta I^{FID}_{FLEX}$, leading to a non-monotonic behavior with k_{ex}. Figure 2 shows how changes in the number and duration of the mixing events influence the relative signal intensity of HetFLEX with respect to HMQC, both when considered on a per-scan as well as on a per-unit-acquisition-time basis. For the illustrated pH and temperature, k_{ex} amounted to approximately 50 Hz, leading to $t_{exch} \approx 40$ ms as the optimum value (Figure 2a). As exemplified by the calculations in Figure S2, this is in agreement with what can be numerically estimated based on the proton transfer ratio [PTR; Equation (1)],[10]

$$PTR = f_s \lambda^{HMQC}[1 - e^{(-k_{ex}t_{exch})}]\frac{1 - e^{-Nt_{prep}/T_1}}{e^{-t_{prep}/T_1} - 1} \quad (1)$$

where f_s is the ratio between the solute and solvent pool concentrations, and λ^{HMQC} is the efficiency of the HMQC transfer. Using the latter as a fixed parameter, Figures 2b and c show how the HetFLEX signal intensity builds up as a function of the number of exchange loops N; note that these data are plotted normalized by both the number of acquisitions and by the unit acquisition time. An exponential increase in intensity occurs as a function of N until $Nt_{prep} \approx T_1^{H_2O}$; the water T_1 thus controls the maximum achievable enhancement, as exemplified by the different plateaus shown in Figure 2b upon increasing the concentration of a relaxation agent. Note that while the absolute HetFLEX enhancements decrease upon reducing the T_1 of water, the fact that Nt_{exch} governs the repetition time of each scan means that shortening the relaxation of water can actually lead to further SNR advantages versus HMQC when viewing the experiment in terms of the acquisition time (Figure 2c). For the chosen $t_{exch} = 40$ ms, for instance, setting $N = 64$ yields approximately 90% of the maximum signal obtained within reasonably short acquisition times. In an additional set of experiments, Figure 2d illustrates how different combinations of t_{exch} and N yielding the same total exchange period of 64×40 ms = 2.56 s modulate the overall HetFLEX intensity. The behavior is clearly non-monotonic, and confirms the existence of an optimum t_{exch} value.

As mentioned, the HetFLEX sequence can be modified to include a second increment, t_2, to encode the ^1H evolution of the NH moieties (Figure 1a). This evolution will modulate the heteronuclear one, leading to the storage of an H_z proton magnetization whose overall dependence will be $\frac{\cos}{\sin}(\omega_N t_1)\frac{\cos}{\sin}(\omega_H t_2)$. As this modulation will be conveyed to the water signal intensity by the exchange process, nested t_1 and t_2 evolutions lead to the possibility of utilizing water to detect 2D-HMQC-like data. Figure 3 exemplifies these solvent-based 2D acquisitions, applied to the amino acids and peptides that were targeted by 1D HetFLEX. Upon

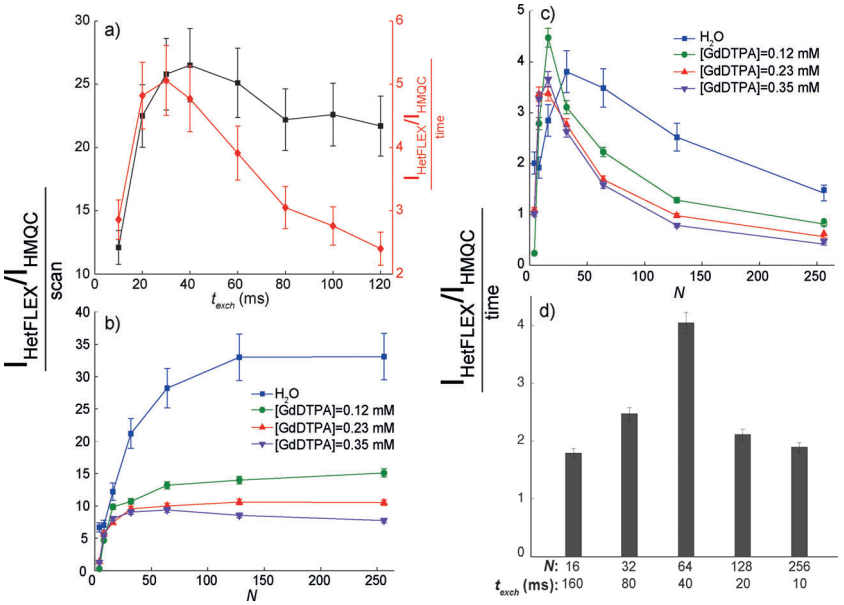

Figure 2. Exploring the effects of different parameters in the Het-FLEX experiment. All data were acquired on a 100 mM ^{15}N-labeled alanine sample in D_2O/H_2O (2:8) at pH 2.2 and $T = 23.5$ °C. a) Calibration of the exchange time employed by the sequence in Figure 1a with 64 t_1 points, $t_2 = 0$, $N = 32$ exchange loops. b, c) Optimization of the number of loops using $t_{exch} = 40$ ms in the presence of varying concentrations of the relaxation agent GdDTPA affecting mostly the T_1 of the solvent. d) Relative intensities obtained using combinations of t_{exch} and N yielding the same total exchange time per scan.

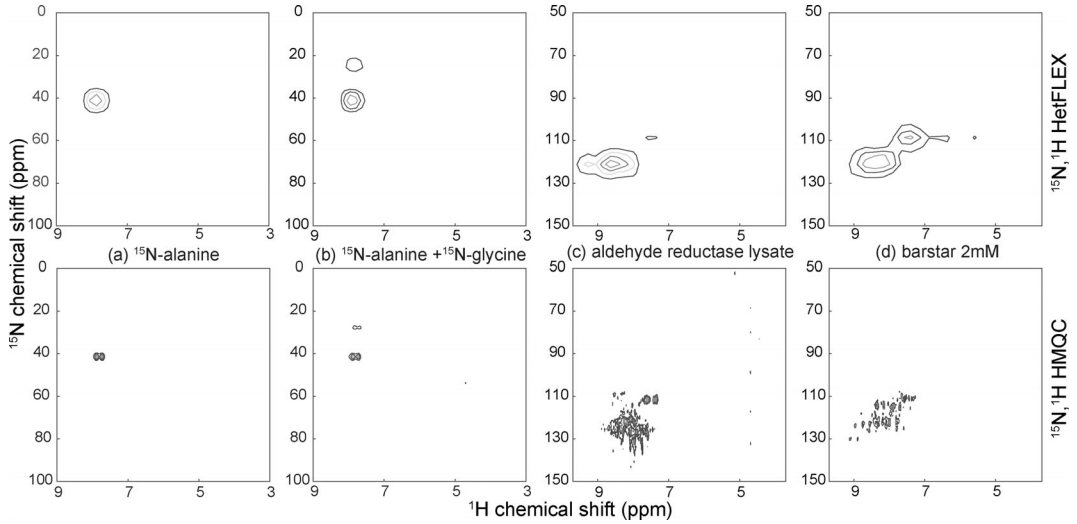

Figure 3. 2D ^{15}N,^{1}H spectra obtained using HetFLEX (top) and HMQC (bottom) on the indicated samples, collected as indicated in Figure 1 a.

comparing these plots with HMQC results (Figure 3, bottom), overall similarities are evident, yet so are major differences. On the one hand, the spectral resolution is worse in the 2D HetFLEX spectra than in their conventional counterparts. This is primarily due to the number of points in the HMQC direct dimension being significantly higher than the one achieved through HetFLEX, which is a consequence of the increased acquisition dimensionality of the latter. Furthermore, as the detection is attained through an exchange process, the experiment is prone to yield broader spectra despite the use of a constant t_{prep} time. On the other hand, although involving the same number of scans, the HetFLEX peaks are approximately two orders of magnitude more intense (in their integrated areas) than their HMQC counterparts. As for the ^{15}N 1D spectra extracted from the 2D HetFLEX version, these are identical to those of the 1D version, apart from an approximately 18-fold increase in intensity arising owing to the extra number of points ($16\,t_2$ increments) used to sample the new additional dimension.

In summary, the applicability of water-detected heteronuclear NMR experiments based on CEST/FLEX propositions has been explored and demonstrated. The approach enables the acquisition of 1D ^{15}N and 2D ^{15}N–^{1}H heteronuclear correlation spectra for cases where the hydrogen atom is in exchange with the aqueous solvent. Among the drawbacks of this method is its relatively slow, indirect detection nature, a feature that fast and ultrafast 2D techniques could solve.[19] Its main advantage lies in the substantial signal amplification that it delivers thanks to its leverage of the abundant water resonance. While the conditions conducive to this fast exchange were created for small molecules by manipulating the pH value, these arose spontaneously under physiological conditions for the studied polypeptides. This opens HetFLEX perspectives for structural and dynamic assessments of disordered biomolecules. A main technical obstacle that we encountered was the concomitant increase in noise associated with the detection of the water resonance; we are currently exploring different options to control this complicating artifact. Another dichotomy that these approaches need to handle concerns the decreasing efficiency of J-based transfers with increased solvent exchange rates versus the increased efficiency of CEST/FLEX with these increasing rates (Table 1). It is clear that in many instances, more involved heteronuclear polarization transfer approaches than HMQC should be adopted to deal with this issue.[20] Other intriguing approaches concern the adaptation of these protocols to include non-labile protons, hyperpolarized systems, or non-aqueous solvents; these and other extensions are currently under investigation.

Acknowledgements

We thank Koby Zibzener for technical assistance and Shira Albeck (ISPC, Weizmann Institute) and Or Szekely for preparing the protein samples. This work was supported by the Kimmel Institute for Magnetic Resonance (Weizmann Institute), Israel Science Foundation Grant 795/13, the Program of the Planning and Budgeting Committee from the Israel Science Foundation (iCORE) Project 1775/12, and the EU Horizon 2020 programme (Marie Sklodowska-Curie Grant 642773).

Conflict of interest

The authors declare no conflict of interest.

Keywords: chemical exchange saturation transfer · frequency-labeled exchange · heteronuclear evolution · HMQC NMR spectroscopy

[1] a) W. W. Brey, A. S. Edison, R. E. Nast, J. R. Rocca, S. Saha, R. S. Withers, *J. Magn. Reson.* **2006**, *179*, 290–293; b) K. Hashi, S. Ohki, S. Matsumoto, G. Nishijima, A. Goto, K. Deguchi, K.

Yamada, T. Noguchi, S. Sakai, M. Takahashi, Y. Yanagisawa, S. Iguchi, T. Yamazaki, H. Maeda, R. Tanaka, T. Nemoto, H. Suematsu, T. Miki, K. Saito, T. Shimizu, *J. Magn. Reson.* **2015**, *256*, 30 – 33.

[2] a) F. Shi, Q. Zhang, P. Wang, H. Sun, J. Wang, X. Rong, M. Chen, C. Ju, F. Reinhard, H. Chen, J. Wrachtrup, J. Wang, J. Du, *Science* **2015**, *347*, 1135 – 1138; b) J. Wrachtrup, A. Finkler, *J. Magn. Reson.* **2016**, *269*, 225 – 236; c) T. Maly, G. T. Debelouchina, V. S. Bajaj, K.-N. N. Hu, C.-G. C.-G. Joo, M. L. Mak-Jurkauskas, J. R. Sirigiri, P. C. A. van der Wel, J. Herzfeld, R. J. Temkin, R. G. Griffin, *J. Chem. Phys.* **2008**, *128*, 052211; d) J. H. Ardenkjaer-Larsen, B. Fridlund, A. Gram, G. Hansson, L. Hansson, M. H. Lerche, R. Servin, M. Thaning, K. Golman, *Proc. Natl. Acad. Sci. USA* **2003**, *100*, 10158 – 10163; e) J. H. Ardenkjaer-Larsen, G. S. Boebinger, A. Comment, S. Duckett, A. S. Edison, F. Engelke, C. Griesinger, R. G. Griffin, C. Hilty, H. Maeda, G. Parigi, T. Prisner, E. Ravera, J. Van Bentum, S. Vega, A. Webb, C. Luchinat, H. Schwalbe, L. Frydman, *Angew. Chem. Int. Ed.* **2015**, *54*, 9162 – 9185; *Angew. Chem.* **2015**, *127*, 9292 – 9317.

[3] a) V. Guivel-Scharen, T. Sinnwell, S. D. Wolff, R. S. Balaban, *J. Magn. Reson.* **1998**, *133*, 36 – 45; b) J. Zhou, J.-F. Payen, D. Wilson, R. Traystman, P. C. M. van Zijl, *Nat. Med.* **2003**, *9*, 1085 – 1090.

[4] a) J. Zhou, P. C. M. van Zijl, *Prog. Nucl. Magn. Reson. Spectrosc.* **2006**, *48*, 109 – 136; b) P. C. M. Van Zijl, N. N. Yadav, *Magn. Reson. Med.* **2011**, *65*, 927 – 948; c) A. D. Sherry, M. Woods, *Annu. Rev. Biomed. Eng.* **2008**, *10*, 391 – 411; d) E. Terreno, D. Delli Castelli, S. Aime, *Contrast Media Mol. Imaging* **2010**, *5*, 78 – 98.

[5] J. Jeener, B. H. Meier, P. Bachmann, R. R. Ernst, *J. Chem. Phys.* **1979**, *71*, 4546 – 4553.

[6] a) K. W. Y. Chan, M. T. McMahon, Y. Kato, G. Liu, J. W. M. Bulte, Z. M. Bhujwalla, D. Artemov, P. C. M. Van Zijl, *Magn. Reson. Med.* **2012**, *68*, 1764 – 1773; b) A. P. Dagher, A. Aletras, P. Choyke, R. S. Balaban, *J. Magn. Reson. Imaging* **2000**, *12*, 745 – 748; c) P. Z. Sun, Y. Murata, J. Lu, X. Wang, E. H. Lo, A. G. Sorensen, *Magn. Reson. Med.* **2008**, *59*, 1175 – 1182; d) B. Yoo, V. R. Sheth, C. M. Howison, M. J. K. Douglas, C. T. Pineda, E. A. Maine, A. F. Baker, M. D. Pagel, *Magn. Reson. Med.* **2014**, *71*, 1221 – 1230; e) D. Delli Castelli, G. Ferrauto, J. C. Cutrin, E. Terreno, S. Aime, *Magn. Reson. Med.* **2014**, *71*, 326 – 332.

[7] F. Kogan, M. Haris, A. Singh, K. Cai, C. Debrosse, R. P. R. Nanga, H. Hariharan, R. Reddy, *Magn. Reson. Med.* **2014**, *71*, 164 – 172.

[8] a) S. D. Swanson, *J. Magn. Reson.* **1991**, *95*, 615 – 618; b) X. Xu, J. S. Lee, A. Jerschow, *Angew. Chem. Int. Ed.* **2013**, *52*, 8281 – 8284; *Angew. Chem.* **2013**, *125*, 8439 – 8442; c) J. Döpfert, M. Zaiss, C. Witte, L. Schröder, *J. Magn. Reson.* **2014**, *243*, 47 – 53; d) Z. Liu, I. E. Dimitrov, R. E. Lenkinski, A. Hajibeigi, E. Vinogradov, *Magn. Reson. Med.* **2016**, *75*, 1875 – 1885.

[9] S. Garcia, L. Chavez, T. J. Lowery, S. I. Han, D. E. Wemmer, A. Pines, *J. Magn. Reson.* **2007**, *184*, 72 – 77.

[10] J. I. Friedman, M. T. McMahon, J. T. Stivers, P. C. M. van Zijl, *J. Am. Chem. Soc.* **2010**, *132*, 1813 – 1815.

[11] N. N. Yadav, C. K. Jones, J. Xu, A. Bar-Shir, A. A. Gilad, M. T. McMahon, P. C. M. van Zijl, *Magn. Reson. Med.* **2012**, *68*, 1048 – 1055.

[12] H. Zeng, J. Xu, N. N. Yadav, M. T. McMahon, B. Harden, D. Frueh, P. C. M. van Zijl, *J. Am. Chem. Soc.* **2016**, *138*, 11136 – 11139.

[13] J. R. Garbow, D. P. Weitekamp, A. Pines, *Chem. Phys. Lett.* **1982**, *93*, 504 – 509.

[14] a) P. Schanda, B. Brutscher, *J. Am. Chem. Soc.* **2005**, *127*, 8014 – 8015; b) S. Grzesiek, A. Bax, *J. Am. Chem. Soc.* **1993**, *115*, 12593 – 12594; c) E. Lescop, P. Schanda, B. Brutscher, *J. Magn. Reson.* **2007**, *187*, 163 – 169; d) L. Müller, *J. Biomol. NMR* **2008**, *42*, 129 – 137.

[15] a) A. F. Mehlkopf, D. Korbee, T. A. Tiggelman, R. Freeman, *J. Magn. Reson.* **1984**, *58*, 315 – 323; b) G. A. Morris, H. Barjat, T. J. Home, *Prog. Nucl. Magn. Reson. Spectrosc.* **1997**, *31*, 197 – 323.

[16] T. Harris, O. Szekely, L. Frydman, *J. Phys. Chem. B* **2014**, *118*, 3281 – 3290.

[17] M. J. Lubienski, M. Bycroft, D. N. M. Jones, A. R. Fersht, *FEBS Lett.* **1993**, *332*, 81 – 87.

[18] D. J. States, R. A. Haberkorn, D. J. Ruben, *J. Magn. Reson.* **1982**, *48*, 286 – 292.

[19] a) A. Tal, L. Frydman, *Prog. Nucl. Magn. Reson. Spectrosc.* **2010**, *57*, 241 – 292; b) M. Mobli, J. C. Hoch, *Prog. Nucl. Magn. Reson. Spectrosc.* **2014**, *83*, 21 – 41; c) K. Kazimierczuk, V. Orekhov, *Magn. Reson. Chem.* **2015**, *53*, 921 – 926.

[20] a) D. P. Frueh, T. Ito, J.-S. Li, G. Wagner, S. J. Glaser, N. Khaneja, *J. Biomol. NMR* **2005**, *32*, 23 – 30; b) T. Yuwen, N. R. Skrynnikov, *J. Biomol. NMR* **2014**, *58*, 175 – 192.

Manuscript received: December 2, 2016
Final Article published: ■■ ■■, ■■■■

Communications

Water-Based NMR Spectroscopy

R. P. Martinho, M. Novakovic,
G. L. Olsen, L. Frydman* ____

Heteronuclear 1D and 2D NMR Resonances Detected by Chemical Exchange Saturation Transfer to Water

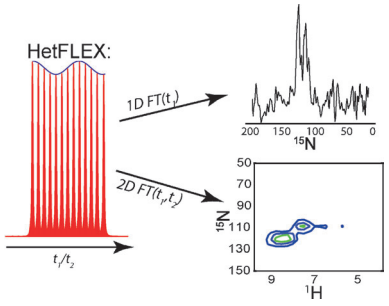

NMR resonances from heteronuclei can be detected through the modulation that they impose on a strong H_2O resonance (shown in red) by combining a 2D heteronuclear NMR sequence with a 2D NMR approach relying on chemical exchange saturation transfer principles (HetFLEX). 1D ^{15}N and 2D $^{1}H/^{15}N$ NMR spectra of small molecules and peptides can be recorded with substantial amplification.